

Analysis of Sweat Evaporation and Heat Transfer on Skin Surface: A Pointwise Numerical Study

Utsav Swarnkar¹, Rabi Pathak² and Rina Maiti³

^{1,2,3} Department of Design and Manufacturing, Indian Institute of Science, Bengaluru, Karnataka, India.
¹utsavs@iisc.ac.in, ²rabipathak@alum.iisc.ac.in, ³rmaiti@iisc.ac.in

Abstract - This study aims to investigate the thermoregulatory role of sweating by comprehensively analysing the evaporation process and its thermal cooling impact on local skin temperature at various time intervals. Traditional experimental methods struggle to fully capture these intricate phenomena. Therefore, numerical simulations play a crucial role in assessing sweat production rates and associated thermal cooling. This research utilizes transient Computational Fluid Dynamics (CFD) to enhance our understanding of the evaporative cooling process on human skin. We conducted simulation employing the k-w SST turbulence model. This simulation includes scenario where sweat evaporation occurs over the skin surface and at particular time interval temperature at different location has been observed and its effect explained. During this study, sweat evaporation was monitored on the skin surface following the commencement of the simulation. Subsequent to the simulation, various observations were made regarding temperature fluctuations at specific points over time intervals. It was noted that points situated closer to the periphery of the droplets exhibited higher levels of heat transfer and lower temperatures, whereas points within the droplets displayed contrasting trends.

Keywords- CFD, Sweat, Evaporation, Multiphase flow, Local heat loss.

Nomenclature and abbreviations

ρ - fluid density	α - volume fraction
q - q^{th} phase	$S_{\alpha q}$ - Source term
\dot{m}_{pq} - Mass Transfer from phase q to phase p	\dot{m}_{qp} - Mass Transfer from phase q to phase p
ϑ - Flow velocity vector field	p - pressure
μ - dynamic viscosity	g - acceleration due to gravity
t - time in Second	E - energy
T - temperature	k_{eff} - Effective thermal conductivity
S_h - Source term	e mass transfer per unit time per unit area
$P_{v,s}$ partial pressure of water vapour at droplet surface	
$P_{v,\infty}$ is partial pressure of water vapour at ambient	ϕ is relative humidity

Introduction

In recent years, there's been a growing emphasis on ensuring that people feel comfortable in buildings, both for their well-being and to manage energy use efficiently. This involves understanding how heat moves around and affects our bodies. We often use a model developed by Fanger[1] to figure out how comfortable people are in different environments. Our bodies have several ways to deal with heat: heat can move through our skin via touch, air currents, and radiation, and we also lose heat through moisture evaporation, like sweating, and breathing. In a typical setting, about three-quarters of our heat loss comes from our skin, and the rest is through sweating. But when we are active or in hot places, sweating becomes more important. Wegner found that when sweat evaporates, it takes a lot of heat away with it [2].

People who live in hot climates, like the tropics, have adapted to handle heat differently. They might start sweating at higher temperatures, but they sweat less overall, which helps them conserve water[3]. Sweat contains salts like sodium and chloride, and losing too much of these can lead to dehydration[4]. Understanding how sweat evaporates and cools our skin is crucial for studying how our bodies regulate temperature. While experiments help, computer simulations,

especially using Computational Fluid Dynamics (CFD) models, give us a deeper insight. Advanced CFD models can predict how sweat evaporates by considering factors like air temperature and movement. They use special techniques to handle the complex interactions between air and moisture, like the Volume-of-Fluid (VOF) method [5,6]. These simulations help us understand how heat flows between our bodies and the environment. By using CFD simulations, we can calculate how much heat moves between our bodies and the air around us. This helps us design spaces that keep people comfortable without wasting energy. We also use different mathematical models to understand how our bodies respond to changing indoor conditions. For example, the $k-\omega$ SST model is good at predicting how air moves in indoor spaces [7,8]. In essence, our study aims to create a CFD model that can accurately predict how heat and moisture move through the air around us. We want to understand how natural air movement affects the temperature of our skin. By doing so, we hope to improve our understanding of how to design spaces that keep people comfortable and healthy.

Methodology

A study conducted at the Indian Institute of Science (IISc) involved 40 students to evaluate thermal comfort levels within an enclosed room. All participants, non-athletes from various regions, were accustomed to the campus environment. Environmental data for computational fluid dynamics (CFD) simulations were obtained from a referenced paper[9]. For CFD simulations, data were acquired for the left arm at an ambient air temperature of 33°C. At this temperature, the initial skin temperature was 34.25°C, chosen to coincide with the onset of active sweating, aligning with the skin temperature. The inner core temperature remained constant at 37.2°C. Relative humidity stood at 48%, with an air velocity of 0.11 m/s [10,11].

A transient simulation was conducted, accounting for heat transfer from the core to the skin surface and heat generation within the skin layers. This process led to a rise in surface temperature, offset by sweat evaporation. The skin, modelled as a 10mm x 10mm x 1.3mm cuboid, disregarded porosity and hair follicles for computational simplicity. It comprised two layers: a constant-temperature core layer and an upper layer with dynamically changing surface temperature. The core temperature was assumed constant at 37.2°C. Thermal conductivity and specific heat capacity of the skin were treated as constants, while sweat was modelled as droplets and layers with a constant rate of 5 microliters. CFD analysis employed Ansys Fluent software, incorporating gravity considerations, and activating the energy equation to capture temperature variations. Turbulence modeling utilized the K-W SST model [16], validated through multiple test cases [12,13,14,15].

To handle multi-phase flow, the Volume-of-Fluid (VOF)[17] method was used, with solver settings meticulously configured based on literature. The simulation mesh comprised 2,879,800 hexahedral elements and 2,716,311 nodes, with a minimum time step of 1e-5. The simulation domain measured 50mm x 30mm x 19mm with one inlet and two outlets. The skin structure consisted of 416,000 hexahedral elements, with each sweat droplet containing 6168 elements for a 0.62 mm radius and 3154 elements for a 0.49 mm radius.

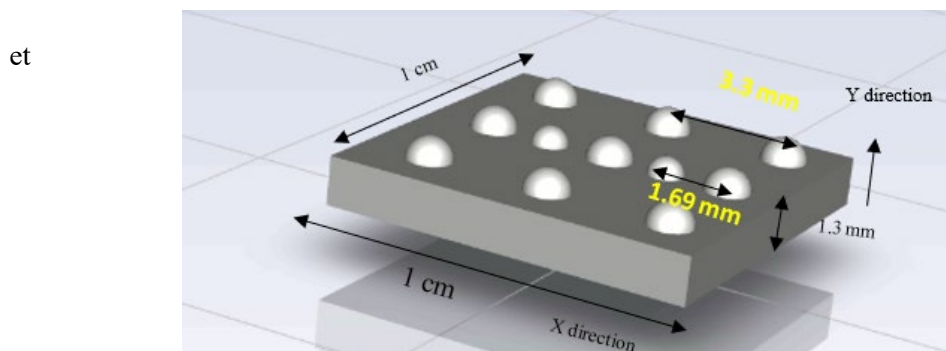


Fig 1 Simulation of a portion of skin in form of cuboid 10 mm (L) × 10 mm (W) × 1.3 mm (H) within a domain of 50 mm (L) × 30 mm (W) × 6.4 mm (H). b) the meshed structure of the cuboid.

The left arm skin domain measured 1cm x 1cm, enclosed within an air envelope. It was divided into two layers: a constant-temperature inner layer and an outer layer influenced by ambient factors. The initial temperature of the upper skin layer matched the onset of active sweating, while the ambient temperature remained at 33°C. Periodic boundary conditions were applied to model adjacent sweat droplets and skin surfaces. The relative humidity within the domain was set at 48%, with heat generation within the skin unit specified as 0.56 watts to accurately simulate internal heat generation processes.

Governing Equations

Continuity Equation: Continuity Equations (eqn 2-4) of the volume fraction are written as follows:[17]

$$\frac{\partial \rho_1 \alpha_1}{\partial t} + \nabla \cdot (\rho_1 \vec{v} \alpha_1) = \dot{m}_1 \quad (1)$$

$$\frac{\partial \rho_2 \alpha_2}{\partial t} + \nabla \cdot (\rho_2 \vec{v} \alpha_2) = \dot{m}_2 \quad (2)$$

$$\dot{m}_1 = -\dot{m}_2 \quad (3)$$

Momentum Equation: The momentum equation (eqn. 5-7) used is as follows:

$$\frac{\partial}{\partial t} (\rho \vec{v}) + \nabla \cdot (\rho \vec{v} \vec{v}) = -\nabla \cdot P + \nabla \cdot [\mu (\nabla \vec{v} + \nabla \vec{v}^T)] + \rho \vec{g} + f_\sigma \quad (4)$$

$$\text{Where, } \rho = \alpha_1 \rho_1 + \alpha_2 \rho_2 \quad (5)$$

$$\mu = \alpha_1 \mu_1 + \alpha_2 \mu_2 \quad (6)$$

In VOF method, single momentum equation is solved where velocity field is shared among the phases. The momentum equation, shown below, is dependent on the volume fractions of all phases through the properties ρ and μ (eqn. 6-7). The variable pressure is calculated using pressure-velocity coupling method by SIMPLE algorithm in the Continuity Equation. The velocity in momentum equation is a combination of mean velocity and fluctuation velocity. The later term is calculated using K-W SST model as follows.

Energy Equation: The equation stated below (eqn. 11) is used to calculate temperature value at each grid point.

$$\frac{\partial}{\partial t} (\rho h) + \nabla \cdot (\vec{v}(\rho h)) = \nabla \cdot (k_{eff} \nabla T) \quad (7)$$

$$h = \frac{\alpha_1 \rho_1 h_1 + \alpha_2 \rho_2 h_2}{\alpha_1 \rho_1 + \alpha_2 \rho_2} \quad (8)$$

Where, K_{eff} denotes thermal conductivity and is calculated using following equation .

$$K_{eff} = \alpha_1 K_1 + \alpha_2 K_2 \quad (9)$$

A purely theoretical and validated formulation proposed by Pauken. the vapour partial pressure difference between the bulk air and the air layer above the droplet surface ($P_{v,s} - \phi P_{v,\infty}$) with surface area available for evaporation (\mathbf{A}) and velocity field (v). This can be done in ANSYS FLUENT by adding source terms to the phase-change model in the governing equations using user-defined functions (UDFs) and the amount of mass transfer ($E_{m,emp}$) can be calculated as follows, given in equation 1.

$$E_{m,emp} = 10^{-6} \times 20.56 + 27.21 v + 6.92 v^2 \left(1 \times 10^{-3} (P_{v,s} - \phi P_{v,\infty}) \right)^{1.22 - 0.19 v + 0.038 v^2} \quad (10)$$

The phase-change processes considered in this article are compressible, turbulent and unsteady two-phase flow and heat transfer problem. In volume-of-fluid (VOF) method (Hirt and Nichols, 1981) it is assumed that sum of volume fractions ($\alpha_1 + \alpha_2$) of all phases equals to 1 in each grid cell.

Table.1. Thermo-physical properties of materials[17].

Sr No	Material Name	Density Kg/m^3	Specific Heat $\text{J/kg-}^\circ\text{C}$	Thermal conductivity W/m-k	Viscosity Ns/m^2	Enthalpy J/kg
1	Air	1.1379	1012	0.024	$1.81 \cdot 10^{-5}$	-
2	water	995.67	4182	0.614	$0.798 \cdot 10^{-3}$	0
3	NaCl	2160	854	6	-	-
4	Skin	1000	3770	0.21	-	-
5	Water Vapor	0.03571683691	1866	0.0186	0.001753	$2561 \cdot 10^3$

Results and discussion

Pointwise Analysis

This figures represent different points on the skin and droplet surface and show the temperature variation with flow time. The points are identified by their respective coordinates in the given figure. Here the flow time is in second, and the temperature is in Kelvin. Here (-) represents the Negative direction.

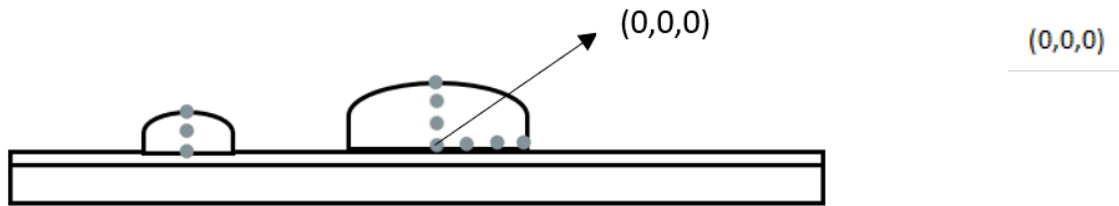


Fig. 2 Schematic diagram of a skin surface with small and big droplet in X-Y plane and their corresponding points over which temperature variation is observed.

Figure 3 illustrates a comparison graph depicting temperature variations at different points within a large droplet. The temperature changes over time in the negative z-direction are highlighted, with coordinates provided in the legend. The initial coordinate point (0,0,0) represents the centre of the large droplet, while the range of points considered extends from the centre to the circumference of the drop. Observations reveal that heat loss is more pronounced at the circumference compared to the centre point, which is surrounded by water. Heat transfer increases progressively with distance from the centre, with molecular heat conduction and vapor-liquid convection playing pivotal roles in droplet evaporation. Notably, the influence of vapor convection emerges as the dominant factor. Points located on the circumference come into direct contact with the air, resulting in heat loss due to both liquid vapor convection and molecular heat conduction [18]. Conversely, only molecular conduction contributes to heat loss at the centre point. Moreover, a local density change occurs from the centre to the circumference of the droplet, leading to a higher temperature gradient at the circumference, as evidenced by the graph.

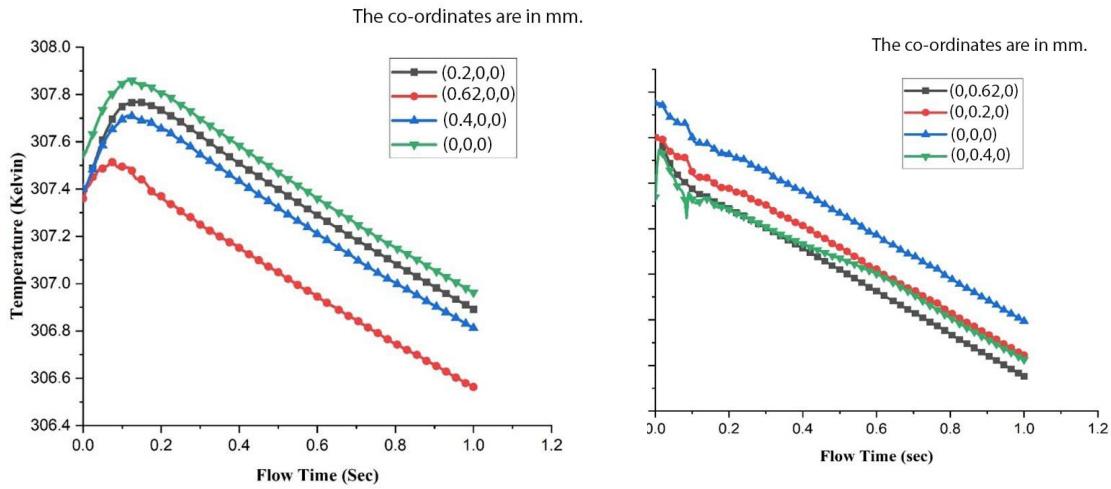


Fig. 3,4 Temperature variation with flow time for different points in the given coordinates in big droplet

Figure 4 illustrates the temperature variation over time at different points in the Y direction within a droplet. Similar to Figure 3, molecular heat conduction and vapor-liquid convection are significant factors contributing to droplet evaporation. The figure highlights that the top point of the droplet surface exhibits the lowest temperature over time. This phenomenon occurs because the top point loses heat to the surrounding air through liquid-vapor evaporation and natural convection [19]. Additionally, the internal flow within the droplet influences the external flow near the droplet due to the higher viscosity of the liquid compared to the air. Conversely, at the bottom centre point where the droplet interfaces with the skin, heat loss occurs solely due to molecular heat conduction. The droplet acts as an obstacle to the flow, resulting in increased heat transfer from the outer surface, particularly at the top point depicted in this figure.

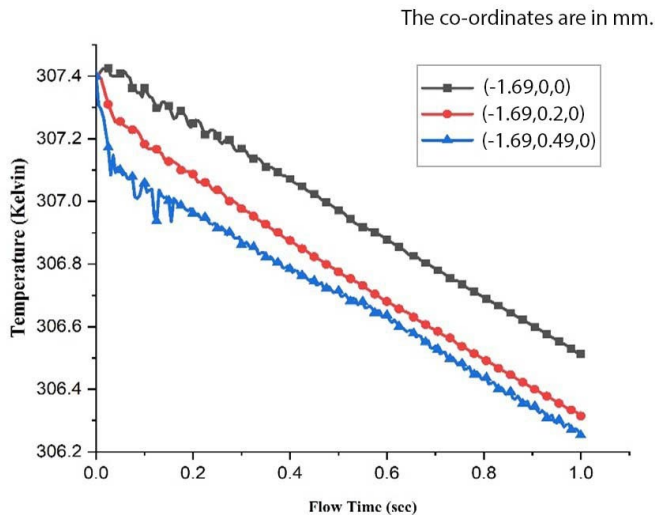


Figure 5 depicts the temperature gradient in small droplets over time.

The graph illustrates that the maximum heat loss occurs at the top point of the droplet, while the minimum heat loss is observed at the bottom point, consistent with the observations made in Figures 14 and 15. The primary mechanism driving heat transfer and evaporation in these droplets involves a combination of shear-induced circulation and gravity-driven flow. Shear-induced circulation is generated due to the inlet velocity, while gravity-driven flows result from temperature gradients. Although both mechanisms contribute, the influence of gravity-driven flow is predominant, particularly given the low velocity of 0.11 m/s applied in the study. The larger surface area of the bigger droplet leads to a higher vapor concentration level, which reduces local concentration gradients and correlated evaporation. Additionally, the shielding effect caused by larger droplets on smaller ones is more pronounced. This creates a recirculating cloud of air around the smaller droplet, consequently increasing the rate of evaporation in the smaller droplet. As a result, the temperature in the smaller droplet is lower compared to the larger droplet [20].

Conclusion

This study presents a comprehensive investigation into the thermoregulatory role of sweating through the analysis of the evaporation process and its thermal cooling impact on local skin temperature at various time intervals. In this study involved conducting transient simulations using the k- ω SST turbulence model to model sweat evaporation occurring over the skin surface. The simulations were conducted incorporating considerations for multi-phase flow using the Volume-of-Fluid (VOF) method and a validated turbulence model. The study utilized Ansys Fluent software to conduct the CFD analysis, with the simulation domain and mesh settings carefully configured to accurately capture temperature variations and heat transfer mechanisms. Results from the simulations revealed significant insights into the heat transfer and evaporation dynamics within sweat droplets on the skin surface. Observations highlighted that heat loss was more pronounced at the circumference of the droplets compared to the center, with molecular heat conduction and vapor-liquid convection playing pivotal roles in droplet evaporation. The influence of vapor convection emerged as the dominant factor driving heat transfer from the droplet surface to the surrounding air. Furthermore, the study elucidated the temperature gradient in small droplets over time, demonstrating that the maximum heat loss occurred at the top point of the droplet, while the minimum heat loss was observed at the bottom point. The primary mechanisms driving heat transfer and evaporation in these droplets involved a combination of shear-induced circulation and gravity-driven flow, with the latter exerting a predominant influence, particularly given the low inlet velocity applied in the study.

References

- [1] P. O. Fanger, *Thermal Comfort – Analysis and Applications in Environmental Engineering*, Robert E. Krieger Publishing Company, Malabar, Florida, 1982.
- [2] L. B. Baker, "Physiology of sweat gland function: The roles of sweating and sweat composition in human health," *Temperature (Austin, Tex.)*, vol. 6, no. 3, pp. 211–259, 2019, doi: 10.1080/23328940.2019.1632145.
- [3] L. E. Armstrong and C. M. Maresh, "Effects of Training, Environment, and Host Factors on the Sweating Response to Exercise," *Int. J. Sports Med.*, vol. 19, no. Suppl. 2, pp. S103–S105, 1998, doi: 10.1055/s-2007-971969.
- [4] Bae, J. S., Lee, J. B., Matsumoto, T., Othman, T., Min, Y. K., & Yang, H. M. (2006). Prolonged residence of temperate natives in the tropics produces a suppression of sweating. *Pflugers Archiv : European journal of physiology*, 453(1), 67–72. <https://doi.org/10.1007/s00424-006-0098-x>.
- [5] W. Hirt and B. D. Nichols, "Volume of Fluid (VOF) Method for the Dynamics of Free Boundaries," *Journal of Computational Physics*, vol. 39, no. 1, pp. 201–225, 1981, doi: 10.1016/0021-9991(81)90145-5.
- [6] S. Osher and R. P. Fedkiw, "Level Set Methods: An Overview and Some Recent Results," *Journal of Computational Physics*, vol. 169, no. 2, pp. 463–502, 2001, doi: 10.1006/jcph.2000.6636.
- [7] A. Stamou and I. Katsiris, "Verification of a CFD Model for Indoor Airflow and Heat Transfer," *Build. Environ.*, vol. 41, no. 9, pp. 1171–1181, 2006, doi: 10.1016/j.buildenv.2005.06.029.

- [8] S. M. A. Aftab, A. S. Mohd Rafie, N. A. Razak, and K. A. Ahmad, "Turbulence Model Selection for Low Reynolds Number Flows," *PLOS ONE*, vol. 11, no. 4, p. e0153755, 2016, doi: 10.1371/journal.pone.0153755.
- [9] R. Maiti, "PMV Model Is Insufficient to Capture Subjective Thermal Response from Indians," *Int. J. Ind. Ergon.*, vol. 44, no. 3, pp. 349–361, 2014, doi: 10.1016/j.ergon.2014.01.005. 9
- [10] L. Lan, Z. J. Zhai, and Z. Lian, "A Two-Part Model for Evaluation of Thermal Neutrality for Sleeping People," *Build. Environ.*, vol. 132, pp. 319–326, 2018, doi: 10.1016/j.buildenv.2018.02.004.
- [11] J. Yang, S. Ni, and W. Weng, "Modelling Heat Transfer and Physiological Responses of Unclothed Human Body in Hot Environment by Coupling CFD Simulation with Thermal Model," *Int. J. Therm. Sci.*, vol. 120, pp. 437–445, 2017, doi: 10.1016/j.ijthermalsci.2017.06.028.
- [12] A. Najjaran, A. Fotoohabadi, and A. R. Shiri, "Determining Heat Transfer Coefficient of Human Body," *Front. Heat Mass Transf.*, vol. 4, 2013, doi: 10.5098/hmt.v4.1.3003.
- [13] Y. Kurazumi and L. Rezgals, "Convective Heat Transfer Coefficients of the Human Body Under Forced Convection from Ceiling," *J. Ergon.*, vol. 04, no. 1, 2014, doi: 10.4172/2165-7556.1000126.
- [14] Fiala, D., Havenith, G., Bröde, P. UTCI-Fiala multi-node model of human heat transfer and temperature regulation. *Int J Biometeorol* **56**, 429–441 (2012). <https://doi.org/10.1007/s00484-011-0424-7>.
- [15] H. Shih, Y.-C. Shih, L.-C. Wang, S.-W. Shiah, and S.-C. Hu, "The model development and case study for transient thermal response of the human body interacting with the coupled fabric-environment system," *Case Studies in Thermal Engineering*, vol. 18, p. 100592, 2020, ISSN: 2214-157X, doi: 10.1016/j.csite.2020.100592.
- [16] F. R. Menter, "Two-Equation Eddy-Viscosity Turbulence Models for Engineering Applications," *A.I.A.A. J.*, vol. 32, no. 8, pp. 1598–1605, 1994, doi: 10.2514/3.12149. 16
- [17] ANSYS Inc., *ANSYS Fluent User's Guide, Release 17.2*, 2016.
- [18] Wang, Z.; Dong, Q.; Zhang, Y.; Wang, J.; Wen, J. Numerical Study on Deformation and Interior Flow of a Droplet Suspended in Viscous Liquid Under Steady Electric Fields. *Adv. Mech. Eng.* **January 2014**, 6. DOI: [10.1155/2014/532797](https://doi.org/10.1155/2014/532797)
- [19] Al-Rawi, Omar, and Mark Wilson. "Influence of Forced Convection on the Evaporation and Internal Dynamics Inside of an Array of Salt Solution Droplets | *MATEC Web of Conferences*, 27 Nov. 2018, doi:10.1051/mateconf/201824001002
- [20] D. Wickert and G. Prokop, "Simulation of Water Evaporation Under Natural Conditions—A State-of-the-Art Overview," *Exp. Comput. Multiph. Flow*, vol. 3, no. 4, pp. 242–249, 2021, doi: 10.1007/s42757-020-0071-5. 20